INSTITUTE OF PHYSICS PUBLISHING JOURNAL OF PHYSICS: CONDENSED MATTER

J. Phys.: Condens. Matter **13** (2001) 1781–1791 www.iop.org/Journals/cm PII: S0953-8984(01)16667-1

Equilibration of stoichiometrically distorted $Fe_{1-x}Al_x(100)$ surfaces

W Meier, V Blum, L Hammer and K Heinz

Lehrstuhl für Festkörperphysik, Universität Erlangen-Nürnberg, Staudtstrasse 7, D-91058 Erlangen, Germany

Received 29 August 2000, in final form 26 January 2001

Abstract

The correlation between segregation kinetics and the geometric and chemical structure of iron-rich $Fe_{1-x}Al_x(100)$ surfaces was investigated for four samples with different bulk stoichiometries ($x = 0.03, 0.15, 0.30, 0.47$) using quantitative low-energy electron diffraction (LEED) and Auger electron spectroscopy (AES). After being largely depleted of Al through preferential sputtering, the surfaces were annealed in a stepwise fashion. Auger signals as well as LEED patterns and intensity spectra were recorded for the transient phases which developed after each step, so monitoring the surfaces' return to equilibrium by means of aluminium segregation. They were used as fingerprints for comparison to the corresponding data of the equilibrium phases which had been analysed quantitatively in earlier investigations. It appears that transient phases of a sample with a certain bulk Al concentration can be identified with equilibrium phases of samples with lower bulk Al content. In other words, the structure of the surface slab accessible by means of LEED and AES is dictated by the actual intermediate slab stoichiometry in accordance with the bulk phase diagram and prevailing local quasi-equilibrium. The intermediate structures are metastable in the sense that the full equilibration of the crystal is kinetically limited by long-range mass transport from the bulk. In contrast, the top layer is always aluminium rich in accordance with the full equilibrium with the surface slab. So, the kinetics observed is dominated by the equilibration between the surface slab and the bulk, a feature possibly applying generally for stoichiometric equilibration in surfaces.

1. Introduction

Most investigations of alloy surfaces deal with well-annealed, i.e. thermal equilibrium states. For ordered or random alloys this means that the focus has mostly been on the equilibrium surface termination and segregational profile. Although cycles of sputtering and annealing are routinely applied for sample preparation—a procedure generally leading to the depletion of one of the constituents in the surface—detailed investigations of the intermediate states of the surface returning to equilibrium as a result of annealing are relatively few (e.g., references

0953-8984/01/091781+11$30.00

[1, 2]). Also, they mostly focus on processes only within the surface, without addressing the problem of the mass transport from deeper regions which is involved. So, a unified picture of the process of compositional equilibration in a surface is as yet lacking. In this paper we attempt to provide such a description for (100)-oriented surfaces of the bcc-based alloy system $Fe_{1-x}Al_x$, using which iron-rich samples of different bulk stoichiometries are considered ($x = 0.03$, 0.15, 0.30, 0.47). Previous studies by AES for $x = 0.15$ [3], 0.20 [4], and 0.47 [5] show that the annealing behaviour of Fe–Al surfaces after preferential sputtering of Al is a well-reproducible process. In the present work, we monitor the samples' return to equilibrium by applying low-energy electron diffraction (LEED) and Auger electron spectroscopy (AES). For $x = 0.47$ we include some earlier results from our group [5–9]. The stoichiometric and geometric structures of the well-annealed equilibrium phases are known due to recent full dynamical LEED analyses [7, 10, 11].

To prepare for what we might have to expect, we recall the bulk phase diagram of Fe–Al [12] in figure 1 as well as the related structural phases in figure 2. For low Al concentrations the A2 phase dominates, with Al and Fe atoms randomly occupying bcc lattice sites according to the actual stoichiometry. For a bulk-terminated (100) surface of such a phase, the corresponding LEED pattern is that of an elemental bcc (100) surface which we define as a (1×1) unit mesh (figure 2(b)). For Al concentrations around 25% and temperatures that are not too elevated, the $D0_3$ structure prevails. Its bulk-terminated (100) surface exhibits a $c(2 \times 2)$ superstructure relative to the bcc (100) surface. For higher Al concentrations the equilibrium structure is of B2 type (CsCl), again with a surface diffraction pattern of (1×1) symmetry.

The bulk concentrations of the four samples investigated in the present paper fall into the different stoichiometry regions described. Whilst the sample with $x = 0.03$ is well within the A2 region, the $x = 0.15$ sample is also in A2 but already comes closer to the $D0_3$ phase

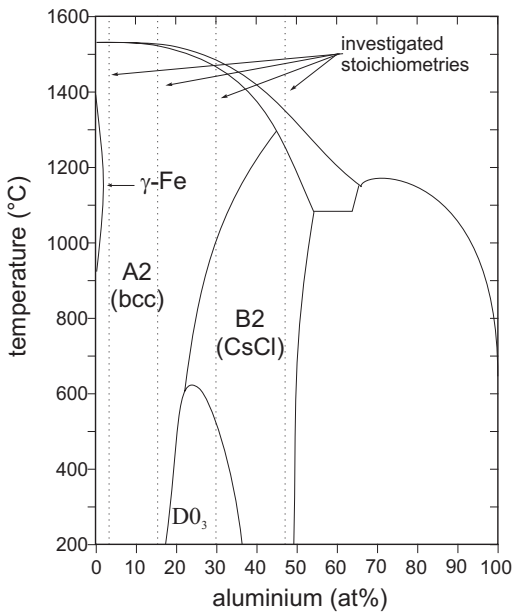

Figure 1. A schematic bulk phase diagram of Fe–Al based on reference [12], illustrating the major phase areas on the Fe-rich side. The stoichiometries investigated in the present paper are indicated by vertical broken lines. Ordered phases on the Al-rich side of the phase diagram are omitted.

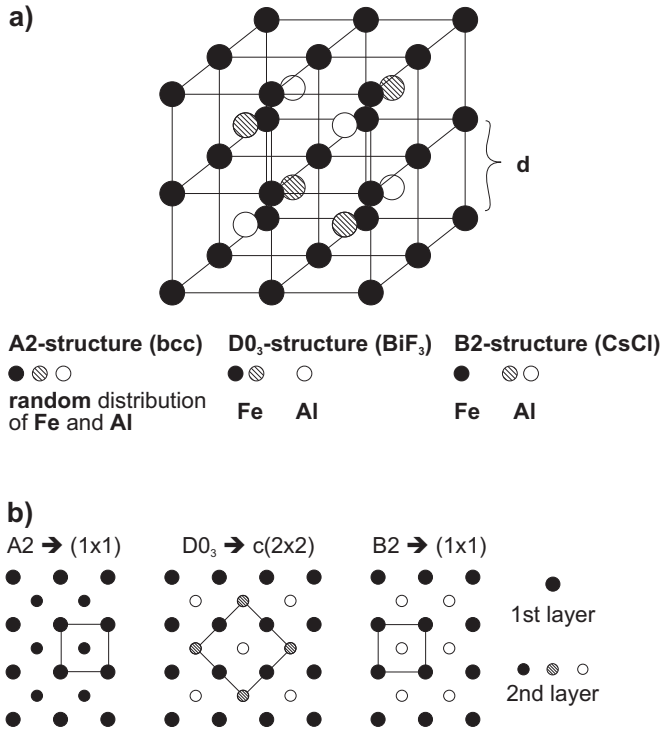

Figure 2. (a) Bulk structures of iron-rich Fe–Al according to the phase diagram in figure 1 and (b) the corresponding structures of the bulk-terminated (100) surfaces

(or the B2 phase at higher temperatures). The sample with $x = 0.30$ is of $D0_3$ type at low temperatures but allows the transition to B2 and/or A2 with increasing temperature. Finally, the sample with the highest Al concentration ($x = 0.47$) lies within the B2 phase up to rather elevated temperatures.

As we aim to monitor the surfaces' structural–stoichiometric development during their return to equilibrium we start from the strongly Al-depleted surface for all samples. Upon annealing, different intermediate states are observed and quantitatively characterized by means of their Auger signals, LEED patterns, and LEED spectra. By comparing these data for the transient structures with those for the known equilibrium phases for samples of very different bulk stoichiometries, we are able to study the interplay of three separate processes: the long-range mass transport necessary to replenish the surface region with Al, the local ordering of the surface region, and the segregation of Al to the topmost atomic layer of the crystal. We will show that for transient phases also, there is always equilibrium between the actual surface and a surface slab below. The structure of the latter is dictated by the intermediate near-surface aluminium concentration according to the bulk phase diagram. These phases are metastable since the full equilibration is still kinetically limited by the necessary long-range mass transport from the bulk.

In the next section we provide details about the sample preparation as well as the LEED and AES measurements. Section 3 recalls the stoichiometric and geometric structure of the equilibrium phases as retrieved in earlier work [7, 10, 11]. Then, the AES and LEED data monitoring the development of the surfaces upon annealing are described. The equilibration process involved is discussed in section 5, which is followed by the conclusions.

2. Experimental procedure

The samples used were provided by the Max-Planck-Institut für Eisenforschung at Düsseldorf (Germany). The (100)-oriented surfaces ($<1^\circ$ accuracy) were *ex situ* mechanically polished (minimum grain size 1 μm). *In situ* cleaning in ultrahigh vacuum (base pressure 2×10^{-11} mbar) was realized through cycles of Ar-ion sputtering and annealing through indirect heating by electron bombardment. Eventually, the samples were flashed to about 1300 K and subsequently sputtered at 400 K (4 min, 2 kV, 10–15 μA cm^{-2} ion current density). This led to a dramatic depletion of Al within the surface as monitored by AES, whereby the elements' low-energy signals were used to provide maximum surface sensitivity (Al: 68 eV; Fe: 47 eV). Starting from that state in each case, the sample was annealed in a stepwise procedure. At each step, the chosen annealing temperature was held constant for a certain time interval Δt with $\Delta t = 2$ min for AES measurements. For LEED $I(E)$ measurements, we chose $\Delta t = 10$ min in order to improve local ordering. After each step, the sample was quenched to about 90 K, where Auger and LEED spectra were taken. In the next step the annealing temperature was increased by 50 K until 1100 K was reached and equilibrium states were assumed in all cases. With further temperature increase (at about 1200 K), preferential evaporation of aluminium sets in. During quenching, the stoichiometry of the surface region is assumed to remain constant as the long-range diffusion of Al is frozen out quickly. For the $Fe_{0.53}Al_{0.47}$ sample this is confirmed by the fact that Auger signals taken for the sample at the annealing temperatures are very close to those for the quenched sample [5].

For the Auger measurements a hemispherical analyser was used. The ratio of peak-to-peak amplitudes, $r(\mathrm{Al/Fe}) = I(\mathrm{Al}_{67\,\mathrm{eV}})/I(\mathrm{Fe}_{47\,\mathrm{eV}})$, was applied to characterize the stoichiometry in the surface region. We do not attempt a quantitative interpretation of the signal as the electron penetration depth is rather uncertain, particularly as regards its variation with the aluminium concentration and the degree of stoichiometric order. The same holds for the matrix factor. Therefore, we use the Auger ratio just as a measure to compare the phases of the different samples.

LEED intensity versus energy spectra, $I(E)$, were taken from a three-grid optics via a computer-controlled video system [13]. Spectra of both integer-order and (when present) fractional-order spots were recorded. Together with the Auger ratio, they serve as structural fingerprints in the present work. Fortunately, it turns out that the spectra of all transient phases of a certain sample are very similar if not identical to those of an equilibrium phase of another sample. As quantitative LEED analyses of all equilibrium phases are available [7, 10, 11] we can easily also identify the transient structures. Therefore, we briefly recall the equilibrium structures in the following section.

3. The structures of the equilibrium phases

The LEED intensities of the equilibrium phases were quantitatively analysed previously and this led to very good theory–experiment fits described by low Pendry R-factors [14], $R_P \leqslant 0.12$ [7, 10]. The best-fit structures for the different samples are schematically displayed in figure 3, where the focus is on the elemental distribution in the top four layers rather than on the geometry (the latter can be found in the literature cited). The stoichiometry below the four layers is bulk-like in each case. For the $x = 0.03$ sample, it appears that there is little difference with respect to a bulk truncated sample except that the actual surface is heavily enriched in Al and practically perfect chemical order is established. The latter corresponds to a c(2×2) overlayer, i.e. the segregation of Al was to a surface sublattice only, so the next-nearest neighbour of an Fe atom is an Al atom and vice versa (the best fit [10] also suggests some

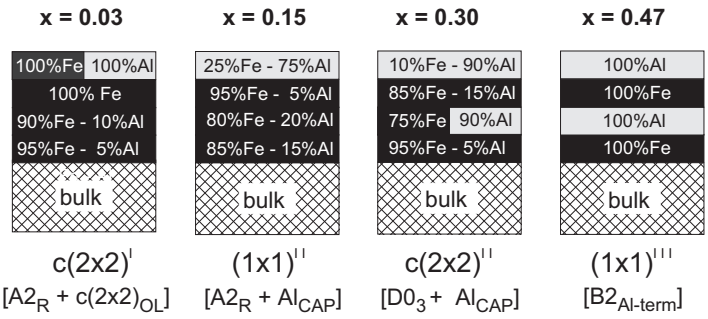

Figure 3. Stoichiometric best-fit models for the different samples according to full dynamical LEED intensity analyses [10, 11]. Split shadings within a layer indicate that two sublattices with the c(2 × 2) symmetry are observed.

order in the third layer, but this is not outside the limits of errors and therefore is neglected here). We denote this phase by $c(2 \times 2)^{I}$ in order to avoid confusion with another phase of this symmetry (see below). For the full surface the notation $A2_R + c(2 \times 2)_{OL}$ can be used, as a c(2 × 2) overlayer (OL) resides on a randomly (R) occupied A2 lattice.

In the equilibrium phase of the $x = 0.15$ surface, even more aluminium segregates to the top layer, so the overlayer superstructure disappears. The phase is denoted as $(1 \times 1)^{II}$, again to differentiate from other such phases, e.g. $(1 \times 1)^{I}$ applying to the as-sputtered surfaces. As a random A2 lattice is capped by an Al-rich layer, the full surface can be described as $A2_R + Al_{CAP}$.

For $x = 0.30$, the bulk structure is $D0_3$ including the structural defects that account for the Al content beyond 25%, but the actual surface is almost completely made up of Al, although such a layer does not exist in the bulk. Below the top layer, the layer sequence is as in the bulk (almost pure Fe layers and mixed layers following each other). Our notation for this structural arrangement is $c(2 \times 2)^{II}$ and the full surface can be described as $D0_3 + Al_{CAP}$.

Finally, the equilibrated surface of the $x = 0.47$ sample is of B2 structure (a slight enrichment of Al in the second layer indicated in earlier work [7] had to be corrected, as it may be explained by parameter correlations [11]). Not surprisingly in view of the other phases, the surface is terminated by Al, so the description $B2_{Al-term}$ can be used. There is no superstructure and we use the notation $(1 \times 1)^{III}$ to avoid confusion with the other phases of (1 × 1) symmetry.

4. Structural development towards equilibrium

The basic phenomena of aluminium depletion by preferential sputtering and the recovery of the overall surface composition upon thermal annealing are well known for transition metal aluminide surfaces, as e.g. reported for FeAl [3, 5, 9, 15], CoAl [16, 17], and NiAl [18–23] surfaces. For the samples investigated in this work, this behaviour is illustrated in figure 4 by displaying the dependence of the above-defined Auger ratio r(Al/Fe) on the annealing temperature, starting with the temperature of sputtering (400 K). Evidently, the curves are qualitatively rather similar for the different samples. There are two plateaus in the low- and high-temperature regimes which correspond to the initially Al-depleted surfaces and the equilibrium state assumed after extensive annealing, respectively (except for $x = 0.47$, where only the high-temperature plateau can be distinguished). The initial depletion level is similar for the $x = 0.03, 0.15$, and 0.30 surfaces, and the equilibrium Al content in the surface increases with the Al bulk concentration as is known from the equilibrium structures described in the last

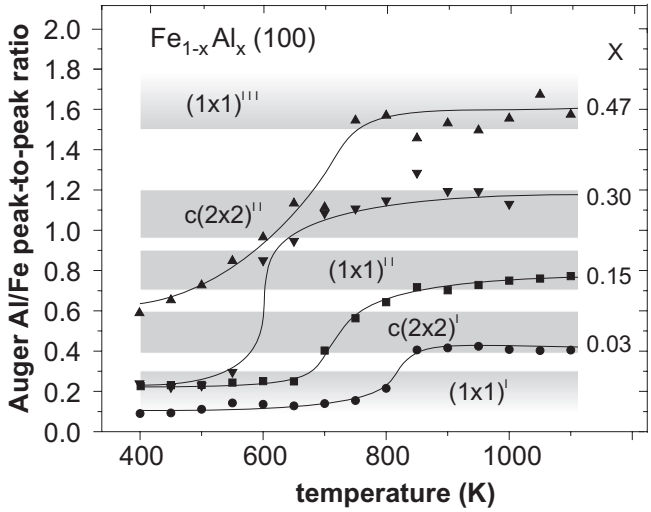

Figure 4. The dependence of the ratio of the peak-to-peak Auger signals $r(\mathrm{Al/Fe}) = I(\mathrm{Al}_{67\,\mathrm{eV}})/I(\mathrm{Fe}_{47\,\mathrm{eV}})$ on the annealing temperature for the four samples investigated (annealing time $\Delta t = 2$ min for each step).

section. In the latter regime, the Al/Fe ratio is largely independent of the annealing temperature up to the point where Al evaporation from the surfaces becomes significant ($T \approx 1200$ K and above [5]). Between the two plateaus there is a transition range which shifts to lower temperatures with increasing x, i.e. the transport of Al to the surface appears to become the easier as the bulk concentration increases (for the $x = 0.47$ sample, segregation seems to be already taking place at 400 K).

On annealing the sputtered $x = 0.03$, 0.15, and 0.30 samples at relatively low temperatures, some structural order develops, as shown by quite intense (1×1) LEED patterns, but broad spots and a substantial background indicate that this order is by no means perfect. The measurement of the corresponding $I(E)$ spectra proves that the underlying structures must be quite similar, including the as-sputtered $x = 0.47$ surface. We therefore denote this phase as $(1 \times 1)^{\mathrm{I}}$. Moreover, these LEED spectra resemble those published for the Fe(100) surface [24], a fact already reported for the sputtered $\mathrm{Fe}_{0.54}\mathrm{Al}_{0.46}(100)$ surface [15]. So, we conclude that the structure of the corresponding surfaces is bcc (A2 structure) with random occupation of the lattice sites by Al and Fe atoms according to the actual stoichiometry within the surface.

As mentioned above, towards higher temperatures the $(1\times1)^{\mathrm{I}}$ phase is bounded by the onset of surface segregation. Of course, the exact onset temperature depends on our experimental timescale, i.e. the annealing time Δt. Still, since we used the same $\Delta t = 2$ min for all AES measurements in figure 4, we may compare the behaviour of the different samples relative to one another. Although a precise quantification is difficult (the AES signal depends too strongly on the exact surface composition profile), the onset temperature of the transition regime generally decreases with rising x and even lies below the sputtering temperature of 400 K for $x = 0.47$. Furthermore, figure 4 suggests that the minimum temperature above which the surface composition does not change any more (i.e. the beginning of the high-temperature plateau) also decreases clearly with bulk Al content up to $x = 0.30$. However, the $x = 0.47$ sample does not adhere to this trend. Certainly, the temperature required for a full equilibration is not lower than for $x = 0.30$, but rather appears to increase again.

In the transition regime itself, the $x = 0.15$, 0.30, and 0.47 surfaces exhibit additional structural phases. However, as is evident from the LEED patterns and intensities recorded, these phases are not new ones, but are structurally identical or at least very similar to the above-mentioned equilibrium structures. Generally, for a sample with a certain value of the Al bulk concentration, we observe as intermediate phases *all* equilibrium phases of the samples with smaller bulk Al concentration. So, as intermediate phase(s) we observe for $x = 0.15$ the $c(2 \times 2)^{I}$ structure, for $x = 0.30$ the $c(2 \times 2)^{I}$ and $(1 \times 1)^{II}$ structures, and for $x = 0.47$ the $c(2 \times 2)^{I}$, $(1 \times 1)^{II}$, and $c(2 \times 2)^{II}$ structures.

To illustrate this behaviour, $I(E)$ spectra of the (10) beam of the $(1 \times 1)^{II}$ phases of the different samples are plotted together in figure 5. The Pendry R-factors [14] used to compare spectra quantitatively and also given in the figure confirm the visual similarity of the curves. This demonstrates that the underlying structures are almost identical, independently of whether they correspond to equilibrium or transition states. This also holds for the other phases, with $R_P < 0.25$ for nominally equal phases of the different surfaces in general. As a demonstration of the structural transition within the same sample, figure 6 displays the development of LEED intensity spectra for selected integer-order and fractional-order spots of $Fe_{0.70}Al_{0.30}(100)$ with the annealing temperature as the parameter. The $I(E)$ spectra undergo clear changes. For instance, the $c(2 \times 2)^{I}$ structure (around 550 K) is markedly different from the $c(2 \times 2)^{II}$ phase (around 700 K).

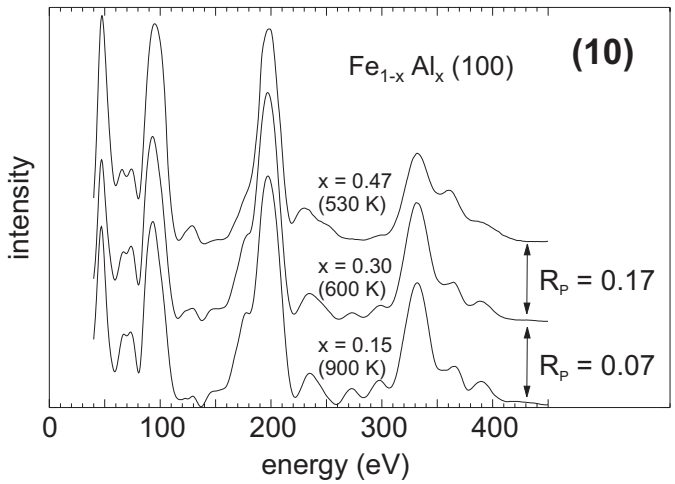

Figure 5. Normalized LEED intensity spectra, $I(E)$, for the (10) beam of the $(1 \times 1)^{II}$ phase for the samples and temperatures indicated (annealing time $\Delta t = 10$ min for each spectrum). Low values of the Pendry R-factor [14] R_P quantitatively confirm the favourable visual comparison of the spectra. The spectrum for $x = 0.30$ corresponds to the 600 K spectrum in the upper frame of figure 6.

We also determined the AES ratio r(Al/Fe) for the different transient superstructures seen in the LEED. As already suggested by the similar $I(E)$ spectra of the phases across different samples, the respective AES ratios also fall into the same range, plotted as horizontal shaded areas in figure 4. In particular, r(Al/Fe) is also characteristic for the surface stoichiometry of the different equilibrium structures, showing that it really does provide a meaningful basis for linking the data of figure 4 (annealing time $\Delta t = 2$ min per step) and LEED data such as those of figures 5 and 6 (annealing time $\Delta t = 10$ min per step). Moreover, this comparison explains a peculiarity observed for the $x = 0.47$ sample. Since, according to figure 4, this

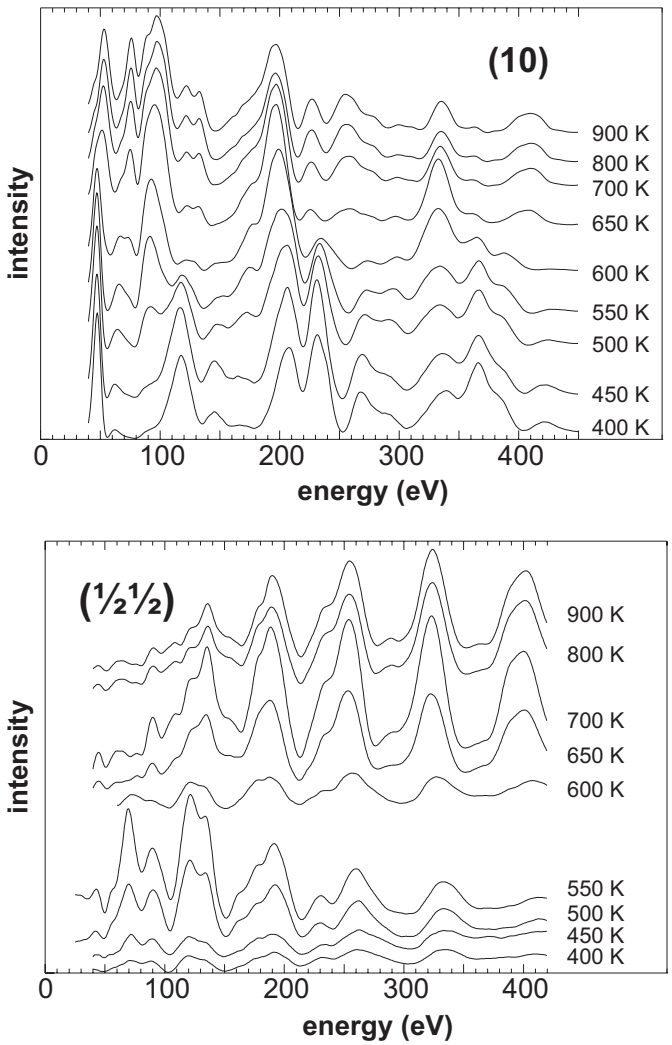

Figure 6. LEED intensity spectra, $I(E)$, for a selected integer-order beam (upper frame) and a selected fractional-order beam (lower frame) of $Fe_{0.70}Al_{0.30}$ with the annealing temperature as the parameter (annealing time $\Delta t = 10$ min for each step). Although the surface shows a (1×1) LEED pattern around 600 K, the diffuse intensity centred about the (1/2, 1/2) position was also measured and is included in the lower frame.

surface is not initially depleted of Al to the same extent as the other samples, its $c(2 \times 2)^{I}$ phase already appears after a short annealing in the range 400–430 K and is only poorly developed in the LEED. Nevertheless, despite the rather faint superstructure spots, we could record their intensity spectra and so clearly identify the structure as $c(2 \times 2)^{I}$.

5. Discussion of the equilibration process

The essential features observed during the development of the surfaces towards thermal equilibrium are:

- There are only five different structural phases. They appear for the same Al near-surface concentration as monitored by AES independently of whether they are equilibrium or (frozen-in) transition phases.
- Below a certain annealing temperature, the surface composition after sputtering does not change within our experimental resolution, and the elemental distribution roughly resembles that of a bulk-truncated A2 random alloy.
- The actual surface, i.e. the top layer of each phase, is enriched in Al compared to the subsurface region both for equilibrium and (frozen-in) transition phases.
- The annealing temperature necessary to produce a certain level of Al surface segregation decreases with the Al bulk concentration.
- The appearance of the different phases is independent of the bulk stoichiometry (as long as the respective near-surface Al concentration can be reached as a result of annealing). The structures within the surface slab below the top layer coincide with those predicted by the volume phase diagram for the corresponding Al concentration (see reference [10]).

These findings can be consistently explained by the following model. Initially, the surface is strongly Al depleted by preferential sputtering. This depletion extends deep into the surface (probably several nm [18], at any rate much deeper than the LEED electron penetration depth), i.e. an Al-depleted *surface slab* forms. In order to fully restore the compositional equilibrium between this surface slab and deeper-lying bulk regions, long-range mass transport is necessary. This long-range diffusion appears to be kinetically limited, so a complete equilibration needs rather elevated annealing temperatures. Once equilibrium has been reached, however, the only clear deviation from bulk stoichiometry and order occurs in the topmost atomic layer which is always enriched in Al [10]. For intermediate temperatures, well-defined transient states of the surface slab develop, although compositional equilibrium with the actual bulk crystal has not yet been attained (i.e. the surface slab itself is still Al depleted). It is the main finding of the present paper that the structure of such intermediate phases for a certain Al concentration within the Al-depleted surface slab is the same as the structure of the sample with the corresponding bulk Al concentration for which complete compositional equilibrium has been attained. So, in principle a single sample with high bulk Al concentration is sufficient for developing all transient structures. The topmost atomic layer is usually enriched in Al compared to the bulk crystal even if the surface slab below is still Fe rich. We can draw two conclusions from this observation:

- In the transition range, the stoichiometry within the surface slab dictates its structure. This is why, below the topmost layer, the latter can be identified with that predicted by the volume phase diagram of the material for the corresponding bulk Al concentration. Of course, this behaviour is facilitated by the fact that the underlying lattice for all phases is of bcc type, and only the corresponding element-specific occupation of sites is required for local quasi-equilibrium.
- In the transition range, the topmost atomic layer is already always in equilibrium with its immediate vicinity (the surface slab), even though the temperature is not sufficient to restore equilibrium between the slab and the bulk. As a consequence, the kinetics observed is dominated by the slab–bulk equilibration rather than by that between the slab and the actual surface.

In total, this suggests a scenario in which the surface structure of the Fe–Al system during equilibration is determined by the interaction of three subsystems: the actual surface (topmost atomic layer), a *surface slab* of limited thickness below, and the bulk. In order to attain a local state of equilibrium between the top layer and the surface slab, only relatively fast short-range diffusion processes (ordering and Al segregation) are required. In contrast, long-range

transport processes are needed to restore the compositional equilibrium between these two combined subsystems and the bulk crystal below. Consequently, this full equilibration takes place on a distinctly longer timescale, and therefore appears to be kinetically limited when compared to the restoration of local order within the surface region itself.

As the AES signal used to characterize the development of the overall surface stoichiometry contains weighted contributions from both the topmost layer and the surface slab below, a more quantitative assessment of the three underlying diffusion regimes (ordering in the surface slab, Al surface segregation, and Al transport from the bulk) is difficult on the basis of these data. Still, our model scenario is at least consistent with the experimental literature on self-diffusion in Fe–Al alloys. Reassuringly, these studies show that bulk ordering phenomena in these materials really occur on timescales similar to those reported here within the same temperature range as the transition regimes which we observe [25, 26]. As mentioned, we find that the temperature above which a full equilibration between the bulk and the surface region is possible decreases noticeably between $x = 0.03$, 0.15, and 0.30, while it appears to rise somewhat when continuing to $x = 0.47$. Of course, we must expect some influence of the larger diffusion distances required for lower bulk concentrations which contributes to the observed trend below $x = 0.30$. Still, it should be noted that a strong decrease in the activation energy for bulk diffusion has indeed been reported for increasing x up to about 0.25 [26]. Consistently, the long-range diffusivity increases clearly with x below $x = 0.25$. In contrast, the literature values for the diffusivity (see reference [27] and references therein) decrease somewhat above $x = 0.25$, i.e. in the $D0_3$ and B2 regions of the phase diagram, which clearly coincides with our observation related to the $x = 0.47$ sample.

Our above model of the equilibration process claims the existence of two different diffusion regimes, i.e. local surface ordering and segregation on the one hand and compositional equilibration with the faraway bulk on the other. Naturally, the question arises of whether both are based on the same atomic-scale diffusion mechanisms. As stated above, the long-range diffusion behaviour which we observe strongly resembles that in the bulk. However, during short-range ordering and Al segregation to the actual surface there may still be contributions from additional diffusion mechanisms, e.g. due to the presence of possibly severe, sputter-induced defects near the onset of the observed transition regime or even the presence of a surface itself. In principle, no such additional mechanisms need be invoked for the $x = 0.03$, 0.15, and 0.30 samples, as the mere difference in required diffusion distance for the two regimes suffices to explain their distinction. However, the situation is different for $x = 0.47$. Here, the onset of the transition regime appears to be lower than for $x = 0.30$, in contrast to the observed higher equilibration temperature; i.e., normal bulk diffusion does not suffice to explain this difference. Still, what exactly causes this behaviour remains unclear.

A final remark concerns the implications of our results for the interpretation of the equilibrium structure of our samples observed after high-temperature annealing and quenching to low temperature. Of course, in thermodynamic equilibrium the observed near-surface order and level of Al segregation to the topmost layer should both depend on temperature. However, our findings show that both phenomena already occur at much lower temperatures than required for compositional equilibrium with the faraway bulk. Thus, on quenching from a high annealing temperature (with quenching times around 2 min), the atoms near the surface initially remain mobile. The near-surface structure that we observe 'in equilibrium' after quenching thus corresponds to the temperature where local diffusion finally freezes out, i.e. somewhere in the transition range of figure 4 for each sample. In line with this conclusion, it proved impossible to preserve the disordered B2 or A2 phases of the $x = 0.30$ sample when quenching down from high annealing temperatures (1000 K)—the sample always showed clear traces of $D0_3$ ordering after cooling.

6. Summary

In summary, by stepwise annealing and freezing out well-defined transient phases, we have been able to provide a direct view of the equilibration kinetics of $Fe_{1-x}Al_x$ (100) surfaces. In principle, a single sample with a high enough bulk Al concentration is sufficient to exhibit all transient phases that appear. There are two regimes of equilibration: first, the formation of equilibrium between the topmost atomic layer and a *surface slab* of limited thickness, and second the long-range compositional equilibration of this surface region with the lower-lying bulk. The latter process leads to intermediate phases of the slab which, though in local quasi-equilibrium according to the phase diagram, are metastable, as full equilibration of the surface is kinetically limited by the necessary long-range mass transport. As a consequence, the kinetics observed is dominated by equilibration between the surface slab and the bulk. Similar intermediate phases have also been reported for other alloy systems [1, 21, 28], so our findings might even be more general.

Acknowledgments

This work was supported by the Deutsche Forschungsgemeinschaft (DFG). We also thank Dr H Viefhaus of the Max-Planck-Institut für Eisenforschung for providing single crystals of excellent quality.

References

[1] Atrei A, Bardi U, Torrini M, Zanazzi E, Rovida G, Kasamura H and Kudo M 1993 *J. Phys.: Condens. Matter* **5** L207
[2] Platzgummer E, Sporn M, Koller R, Forsthuber S, Schmid M, Hofer W and Varga P 1999 *Surf. Sci.* **419** 236
[3] Eltester B, Uebing C, Viefhaus H and Grabke H J 1997 *Fresenius J. Anal. Chem.* **358** 196
[4] Gemmaz M, Afyouni M and Mosser A 1990 *Surf. Sci.* **227** L109
[5] Graupner H, Hammer L, Müller K and Zehner D M 1995 *Surf. Sci.* **322** 103
[6] Graupner H 1995 *Thesis* Universität Erlangen-Nürnberg
[7] Kottcke M, Graupner H, Zehner D M, Hammer L and Heinz K 1996 *Phys. Rev.* B **54** R5275
[8] Kottcke M 1997 *Thesis* Universität Erlangen-Nürnberg
[9] Hammer L, Graupner H, Blum V, Heinz K, Ownby G W and Zehner D M 1998 *Surf. Sci.* **412/413** 69
[10] Blum V, Meier W, Hammer L, Heinz K, Schmid M, Lundgren E and Varga P 2001 *Surf. Sci.* **474** 81
[11] Blum V, Hammer L, Meier W and Heinz K 2001 *Surf. Sci.* submitted
[12] Predel B 1991 *Landolt–Börnstein New Series* Group IV, vol 5a (Berlin: Springer)
[13] Heinz K 1988 *Prog. Surf. Sci.* **27** 239
[14] Pendry J B 1980 *J. Phys. C: Solid State Phys.* **13** 937
[15] Wang C P, Jona F, Gleason N R, Strongin D R and Marcus P M 1993 *Surf. Sci.* **298** 114
[16] Mrozek P, Menyhard M, Wernisch J and Jablonski A 1984 *Phys. Status Solidi* a **84** 39
[17] Blum V, Rath C, Castro G R, Kottcke M, Hammer L and Heinz K 1996 *Surf. Rev. Lett.* **3** 1409
[18] Thomas M P and Ralph B 1983 *Surf. Sci.* **124** 151
[19] Davis H L and Noonan J R 1985 *J. Vac. Sci. Technol.* A **3** 1507
[20] Noonan J R and Davis H L 1987 *Phys. Rev. Lett.* **59** 1714
[21] Mullins D R and Overbury S H 1988 *Surf. Sci.* **199** 141
[22] Mrozek P and Jablonski A 1989 *Surf. Sci.* **208** 351
[23] Blum R P, Ahlbehrendt D and Niehus H 1996 *Surf. Sci.* **366** 107
[24] Wang Z Q, Li Y S, Jona F and Marcus P M 1987 *Solid State Commun.* **61** 623
[25] Lawley A and Cahn R W 1961 *J. Phys. Chem. Solids* **20** 204
[26] Vennegues P, Cadeville M C, Pierron-Bohnes V and Afyouni M 1990 *Acta Metall. Mater.* **38** 2199
[27] Helander T and Agren J 1999 *Acta Mater.* **47** 1141
[28] Wang C P, Kim S K, Jona F, Strongin D R, Sheu B-R and Marcus P M 1995 *Surf. Rev. Lett.* **2** 183